Adaptive algorithms for aperiodic dielectric structures

The study of photonic crystals (PCs) is inspired, in part, by a desire to seek new compact designs for optical and RF components. Much work has focused on two-dimensional (2D) periodic dielectric structures because of the availability of planar fabrication techniques. However, there are a number of fundamental issues that appear to be barriers to adoption of PCs as a technology. These include the fact that the inherent spatial periodicity of the PC structure results in limited functionality. Often one must break spatial symmetry to obtain a useful device response. For example, wave-guides are typically created by introducing a line-defect and filters might make use of one or more point defects. Hence, one may make the observation that usually a desired functionality requires breaking the underlying spatial symmetry of the periodic dielectric structure. Even in situations where one wishes to access properties intrinsic to periodic dielectrics such as non-linear dispersion, coupling electromagnetic radiation from free-space and finite-size effects present significant challenges.

One approach that attempts to circumvent such difficulties is application of optimization techniques to PCs. On the one hand, such numerical studies are usually limited to a finite number of identical dielectric scatters whose broken symmetry spatial distribution is restricted to periodic PC lattice positions. On the other hand, they benefit from the fact that a less biased search of solution space can result in non-intuitive optimized designs. Our approach has been to retain identical dielectric scatters but to remove all bias to periodic PC inspired designs. In this way adaptive algorithms can seek optimal solutions in a much larger space of *aperiodic* dielectric structures and hence, at least in principle, access a larger range of functionalities.

Laboratory measurements were performed using mm-wave electromagnetic (EM) radiation at frequency f_0 = 37.5 GHz corresponding to free-space wavelength λ_0 = 8 mm. Because electromagnetic waves scattering from non-magnetic lossless dielectric is determined by the Helmholtz equation, our approach scales with frequency and hence may be directly applied to the design of nanophotonic devices.

For our prototype problem we are interested in EM power distribution on a measurement surface. Even though the objective response is specified in a limited region of the device, the forward problem is solved over the entire modeling domain. The quasi-2D geometry of typical PCs as well as efficiency considerations led us to implement a 2D EM field solver. Our experiments performed at mm-wave frequencies also use a 2D geometry. Fig. 1(a) shows the basic experimental arrangement in which a f_0 = 37.5 GHz RF signal is introduced into a wave guide whose 7 mm × 3.5 mm aperture is attached to a metal horn. The EM power distribution is detected using a probe that can move to angle θ on a radius r_s = 60 mm. This defines a measurement surface, *s*. To maintain the 2D nature of the EM experiment, the total structure is sandwiched between two metal plates separated by 3.5 mm < $\lambda_0/2$. The prototype problem we choose to study has an objective response in which the incident EM radiation propagating in the $\theta = 0^o$ direction is scattered into a top hat function whose peak on the measurement surface occurs over the angular range $30^o \le \theta \le 60^o$.

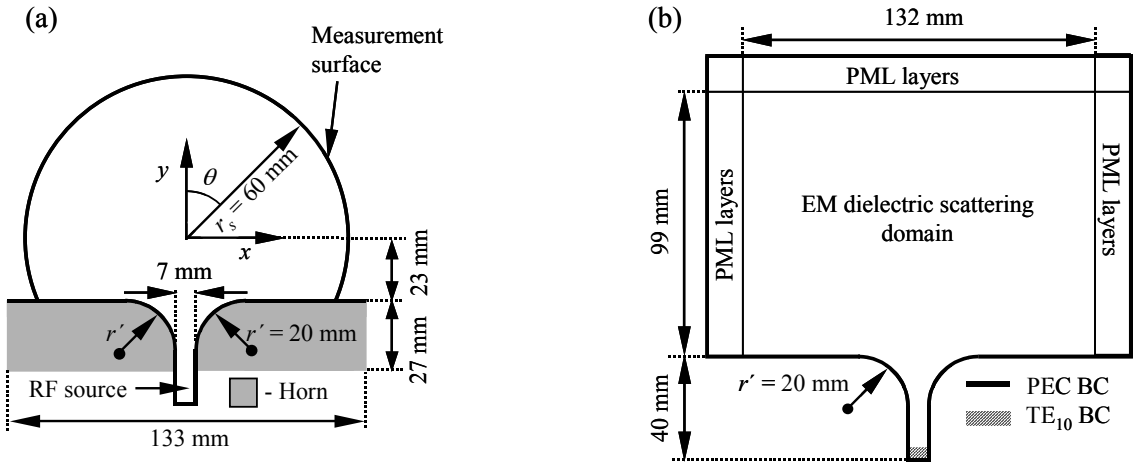

Fig. 1. (a) Top view of experimental layout showing physical dimensions. EM power from a RF source of frequency f_0 = 37.5 GHz is fed via a wave-guide and horn. The measurement surface is indicated. In the experiments, EM power is measured as a function of θ on this surface. (b) Domain decomposition of the FD EM simulation. PML layers of finite thickness are truncated with a PEC boundary condition. The wave-guide introduces the EM-beam as a fixed TE_{10} mode EM-field on the indicated boundary.

The forward problem we consider describes the propagation of the EM-wave over the domain illustrated in Fig. 1(b). This EM dielectric scattering domain contains the dielectric scatters whose spatial arrangement we wish to optimize. Since stationary solutions at a single frequency are sought we consider Maxwell's equations in the frequency domain, eliminating the time variable. When only dielectric material is present and no currents flow, Maxwell's equations simplify further. The magnetic field can be eliminated to yield:

$$\nabla\times\left(\mu_0\mu_{\mathrm{r}}\right)^{-1}\cdot\nabla\times\mathbf{E}-\omega_0^2\varepsilon_0\varepsilon_{\mathrm{r}}\mathbf{E}=0 \tag{1}$$

where **E** is the electric field, $\omega_0 = 2\pi f_0$, ε_0 is the permittivity of free-space, ε_{r} is relative permittivity, μ_0 is the permeability of free-space, and μ_{r} is the relative permeability.

We have verified our numerical simulations by performing experiments. As an initial test, a 5 × 5 finite-sized periodic array of cylindrical dielectric scatters with lattice constant equal to the free-space wavelength, λ_0, was studied. Figure 2(a) is a photograph of 25 Teflon cylinders arranged in a 5 × 5 finite-sized periodic array and attached to a metal slab that forms the lower half of a wave-guide. The Teflon cylinders have a measured diameter of 3.175 ± 0.025 mm and $\varepsilon_{r_z} = 2.05$. Experiments to measure EM power were performed with the upper half of the metal wave-guide attached. EM power reaching the measurement surface was detected using a small dipole antenna feeding a narrow-band amplifier.

Figure 2(b) shows the calculated power distribution at frequency f_0 = 37.5 GHz. In the Fig., the gray scale indicates relative EM power measured in units of dB. The calculations show a diffraction pattern that is symmetric about the $\theta = 0^{\mathrm{o}}$ line. This is to be expected for the periodic

array. In addition, there is interference between EM waves emanating from the dielectric array and subsequently reflected from the metal horn.

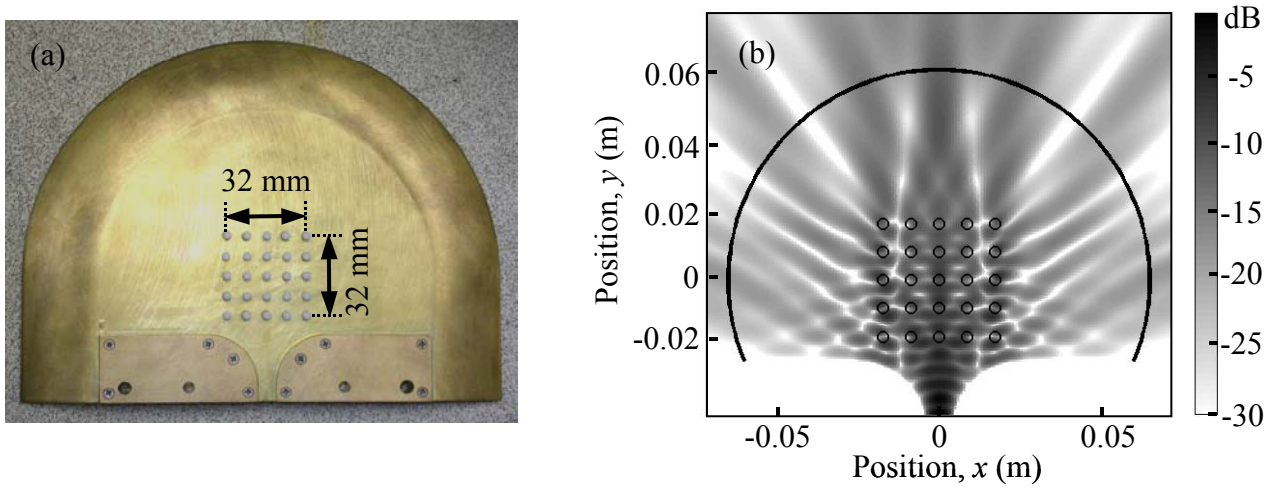

Fig. 2. (a) Photograph showing top view of 25 Teflon cylinders arranged in a 5 × 5 finite-sized periodic array and attached to a metal slab that forms the lower half of a wave-guide. The upper metal plate of the EM wave-guide is removed. (b) Calculated relative EM power at frequency f_0 = 37.5 GHz in the dielectric scattering domain. The gray scale is in dB. EM radiation emerging from the metal horn is incident on a 5 × 5 finite-sized lattice of dielectric cylinders. The dielectric cylinders are 3.175 ± 0.025 mm in diameter and are placed symmetrically about the origin with lattice spacing λ_0. The relative permittivitty of the Teflon cylinders is $\varepsilon_r = 2.05$. The solid line is the measurement surface.

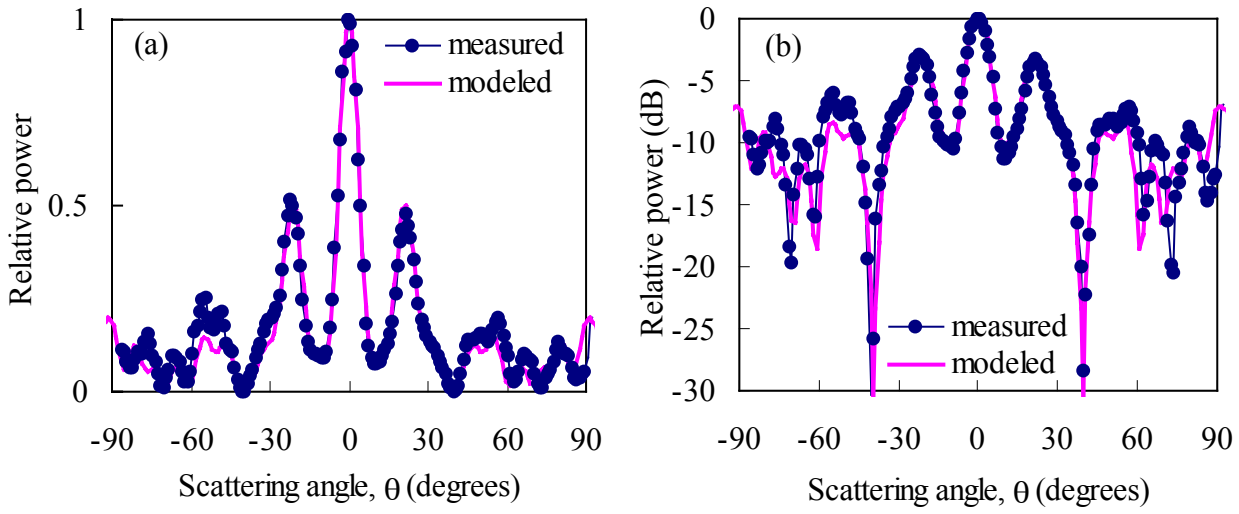

Fig. 3. (a) Calculated and detected relative EM power as a function of angle θ on the measurement surface. (b) Same as (a) but relative power is on a logarithmic scale (dB).

Figure 3(a) shows a comparison between calculated and detected EM power as a function of angle θ on the measurement surface, *s*. The relative power scale is linear. As may be seen,

agreement between calculated and measured data is good with all the main features in appearing in both data. Figure 3(b) is the same data as in (a) but with relative EM power plotted on a logarithmic scale. Here, the excellent agreement for the three main peaks and the –30 dB minima at $\pm$ 40° is apparent. A slight asymmetry in the measured data also exists whose origin is likely due to dielectric cylinder placement.

As our prototype problem we sought an objective response in which the maximum amount of incident EM radiation propagating in the $\theta = 0^{o}$ direction is scattered into a top hat function defined on the measurement surface in Fig. 1(a) and whose peak occurs in the angular range $30^{o} \le \theta \le 60^{o}$. Symmetrically placed structures are unable to provide the desired functionality. However, one anticipates broken symmetry spatial arrangements of dielectric scatters to do better.

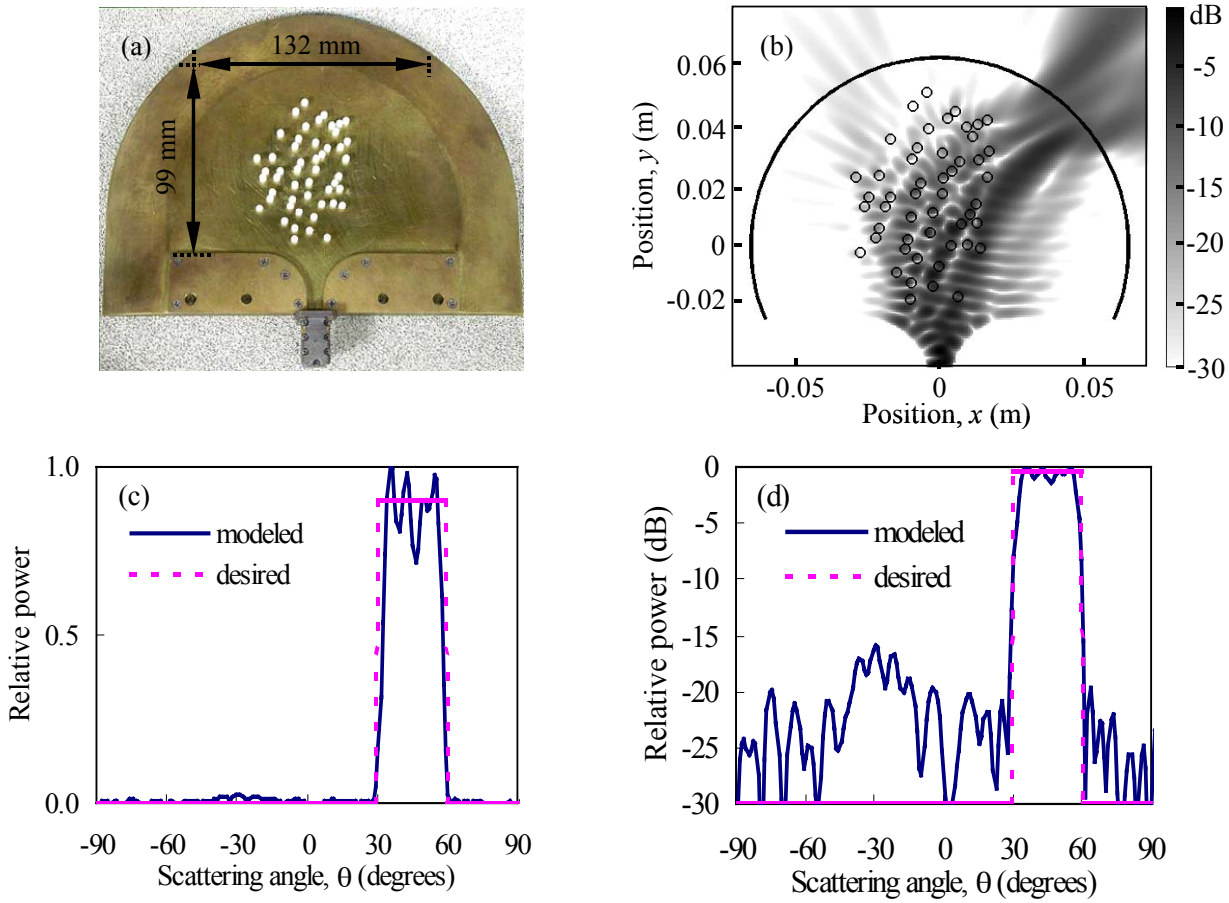

Fig. 4. (a) Photograph showing top view of aperiodic dielectric array attached to lower metal plate that forms the lower half of an EM wave-guide. The upper metal plate of the EM wave-guide is removed. (b) Calculated relative EM power at frequency f_0 = 37.5 GHz. The gray scale is in units of dB. EM radiation from the metal horn is incident on 50 dielectric cylinders in the dielectric scattering domain. The dielectric cylinders are 3.175 $\pm$ 0.025 mm in diameter and ε_r = 2.05. The cylinder positions are optimized to focus EM power on the measurement surface under a top-hat function which peaks between angles $30° \le \theta \le 60°$. The measurement surface is shown as a solid line. (c) The desired and modeled power profile along the measurement surface. 95% of the calculated EM power reaching the measurement surface is focused under the top-hat peak. The ripples in the top-hat's power as a function of θ are 1.45 dB peak-to-peak. (d) Same as (c) but power is on a logarithmic scale (dB).

Rather than attempt to adapt ad-hoc PC-inspired designs, we used the search algorithm to find the optimal spatial configuration of 50 identical Teflon dielectric cylinders. The result was a non-intuitive aperiodic distribution. Figure 4(a) is a photograph of the experimental arrangement showing a top view with upper metal plate removed. As may be seen, the positions of the Teflon cylinders do not have any obvious spatial symmetry. Figure 4(b) shows the calculated relative EM power at frequency f_0 = 37.5 GHz. The gray scale is in dB and the solid line is the measurement surface. EM radiation from the metal horn is incident on the 50 dielectric cylinders in the dielectric scattering domain. Figure 4(c) shows the desired (broken curve) and modeled (solid curve) power profile along the measurement surface. 95.0% of the calculated EM power reaching the measurement surface in the angular range $-90^o \le \theta \le 90^o$ is focused under the $30^o \le \theta \le 60^o$ top-hat peak. The ripples in the top-hat's power as a function of θ are 1.45 dB peak-to-peak. Figure 4(d) is the same as (c) but power is on a logarithmic scale (dB).

Figure 5(a) shows calculated and detected relative EM power profile along the measurement surface. Figure 5(b) is the same as (a) but the relative power scale is logarithmic and measured in dB. Ripples at the top-hat peak are approximately 1.77 dB peak-to-peak. This is only 0.32 dB greater than the calculated value. The portion of the measured power focused between scattering angles $30^o \le \theta \le 60^o$ in the range $-90^o \le \theta \le 90^o$ is 92.4%. This is slightly less than the calculated value of 95.0%.

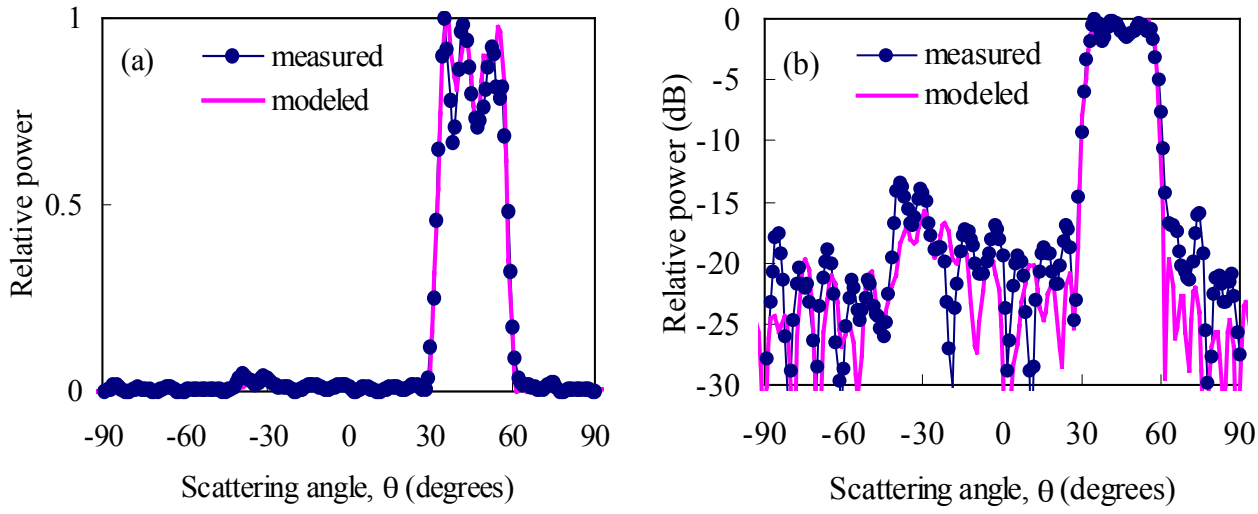

Fig. 5. (a) Calculated and measured EM power profile along measurement surface. The relative power scale is linear. (b) Same as (a) but power scale is in dB. Ripples at the top-hat peak are approximately 1.77 dB peak-to-peak. The portion of the measured power focused between scattering angles $30° \le \theta \le 60°$ in the range $-90° \le \theta \le 90°$ is 92.37%.